Electronic Supplementary Information

Second harmonic generation in 2D moiré superlattices composed of bilayer transition metal dichalcogenides

Xiaoyu Yang[a], Xinjiang Wang[a], Muhammad Faizan[a], Xin He[*a], and Lijun Zhang[*a]

[a] State Key Laboratory of Integrated Optoelectronics, Key Laboratory of Automobile Materials of MOE, and School of Materials Science and Engineering, Jilin University, Changchun 130012, China.

*Address correspondence to: lijun_zhang@jlu.edu.cn and xin_he@jlu.edu.cn

Calculation methods of SHG susceptibility

The SHG susceptibility tensor $\chi^{abc}_{total}(2\omega,\omega,\omega)$ can be calculated as the sum of interband transitions $\chi^{abc}_{inter}(2\omega,\omega,\omega)$, the intraband transitions $\chi^{abc}_{intra}(2\omega,\omega,\omega)$, and the modulation of interband terms by intraband terms $\chi^{abc}_{mod}(2\omega,\omega,\omega)$, written as[1]

$$\chi^{abc}_{total}(2\omega,\omega,\omega)=\chi^{abc}_{inter}(2\omega,\omega,\omega)+\chi^{abc}_{intra}(2\omega,\omega,\omega)+\chi^{abc}_{mod}(2\omega,\omega,\omega) \quad (1)$$

each term in this formula can be written as

$$\chi^{abc}_{inter}(2\omega,\omega,\omega)=\frac{1}{\Omega}\sum'_{nmlk}W_k\times\left\{\frac{2r^a_{nm}\{r^b_{ml}r^c_{ln}\}}{(\omega_{ln}-\omega_{ml})(\omega_{mn}-2\omega)}-\frac{1}{\omega_{mn}-\omega}\left[\frac{r^c_{lm}\{r^a_{mn}r^b_{nl}\}}{(\omega_{nl}-\omega_{mn})}-\frac{r^b_{nl}\{r^c_{lm}r^a_{mn}\}}{(\omega_{lm}-\omega_{mn})}\right]\right\} \quad (2)$$

$$\chi^{abc}_{intra}(2\omega,\omega,\omega)=\frac{1}{\Omega}\sum_k W_k\times\left\{\sum'_{nml}\frac{\omega^{-2}_{mn}}{(\omega_{mn}-\omega)}\times\left[\omega_{ln}r^b_{nl}\{r^c_{lm}r^a_{mn}\}-\omega_{ml}r^c_{lm}\{r^a_{mn}r^b_{nl}\}\right]-\right.$$
$$\left.8i\sum'_{nm}\frac{1}{\omega^2_{mn}(\omega_{mn}-2\omega)}r^a_{nm}\{\Delta^b_{mn}\gamma^c_{ln}\}+2\sum'_{nml}\frac{r^a_{nm}\{r^b_{ml}r^c_{ln}\}(\omega_{ml}-\omega_{ln})}{\omega^2_{mn}(\omega_{mn}-2\omega)}\right\} \quad (3)$$

$$\chi^{abc}_{mod}(2\omega,\omega,\omega)=\frac{1}{2\Omega}\sum_k W_k\left\{\sum_{nml}\frac{1}{\omega^2_{mn}(\omega_{mn}-\omega)}\times\left[\omega_{nl}r^a_{lm}\{r^b_{mn}r^c_{nl}\}-\omega_{lm}r^a_{nl}\{r^b_{lm}r^c_{mn}\}\right]-i\sum_{nm}\frac{r^a_{nm}\{r^b_{mn}\Delta^c_{mn}\}}{\omega^2_{mn}(\omega_{mn}-\omega)}\right\} \quad (4)$$

In these formulas, a, b, c denotes the direction of tensor. ω denotes the photon energy. Ω is the volume of crystal cell. W_k is the weight of the k point. n,m,l denotes the valence states, conduction states, and the third states, respectively. Thus, for example, ω_{ln} denotes the energy between band l and band n that is calculated by $\omega_l - \omega_n$. r is the position matrix elements and r_{nm}^a denotes the matrix element between band n and band m in direction a.

The determination of crystal cell volume Ω is crucial for accurate SHG calculations. However, in the case of 2D materials with a vacuum layer, defining their volume becomes ambiguous. To address this issue, we adopt the concept of effective volume in this study, which serves as an approximation for the volume of bilayer structure in the bulk material (the left graph). The effective volume is defined as the product of the in-plane area S of the unit cell and the effective thickness. The effective thickness is obtained by summing the interlayer distance L in the bilayer lattice and the thickness h of the bilayer TMD, as illustrated in the figure below. For the monolayers in this work, their thickness h are consider as the interatomic distance between chalcogen atoms. We define the effective volume in this way so that the results can be generalized to the bulk phase material (the results can be compared with the bulk phase material). Because $h + L =$ lattice parameter C (the right graph).

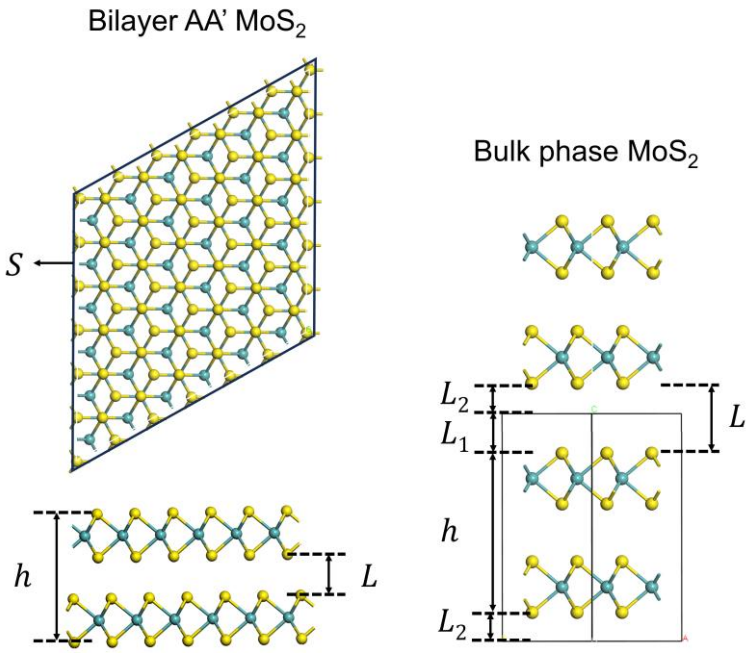

Therefore, the effective volume Ω_{eff} can be written as

$$\Omega_{eff} = S \times (L + h) \tag{5}$$

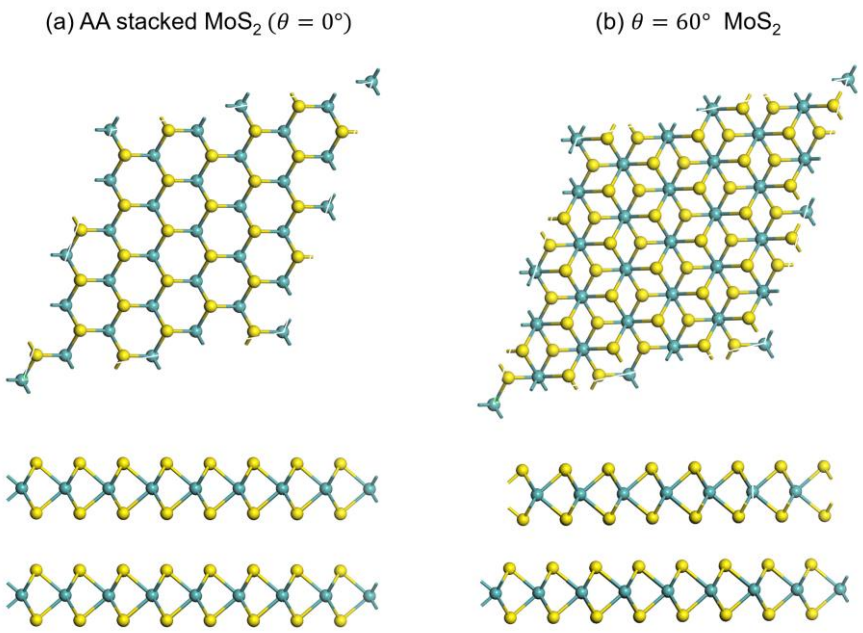

Figure S1. The crystal structure of AA stacked MoS_2 and θ=60° MoS_2. The blue and yellow ball represents Mo and S atom.

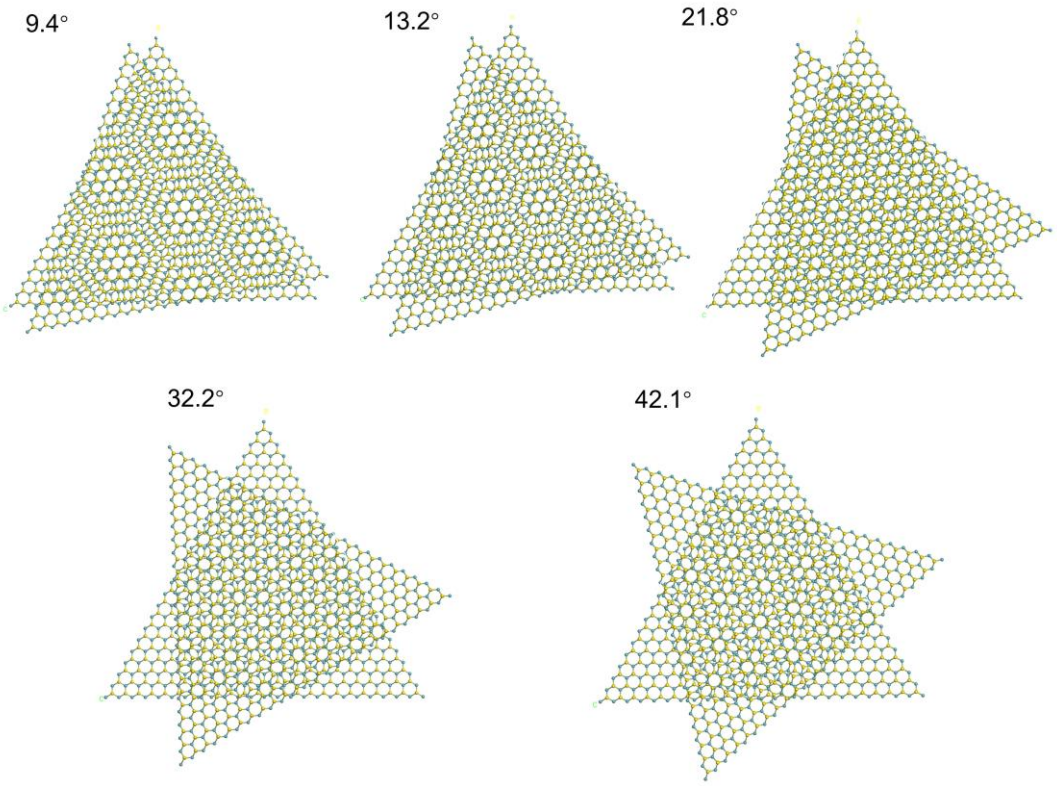

Figure S2. The relaxed crystal geometry of TMD MSLs with different twist-angles. MSL with different twist-angle has different Moiré pattern.

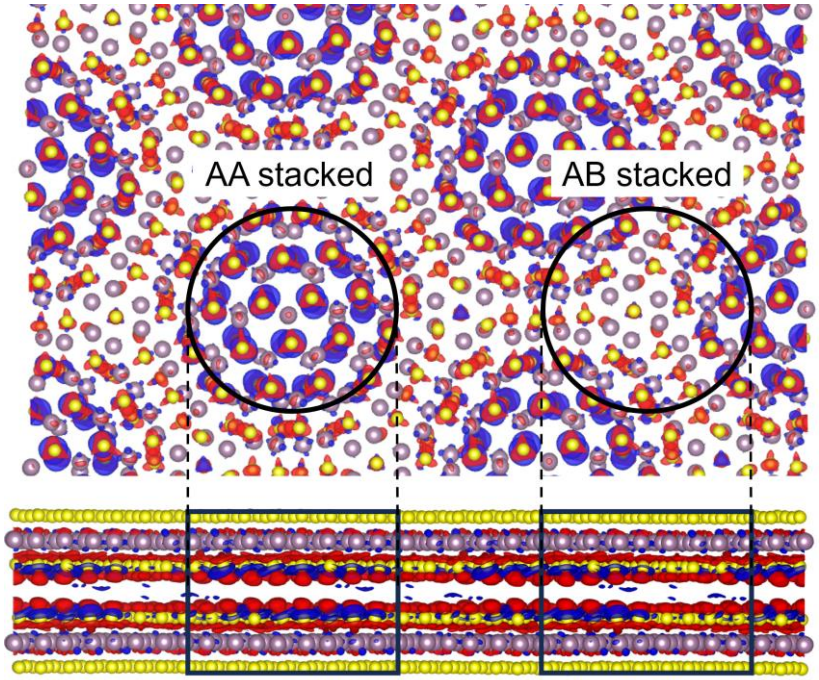

Figure S3. The interlayer charge transfer of 9.4° MoS_2. AA stacked means that Mo(S) is aligned with the same type of atom in the c direction. AB stack indicates that Mo(S) is aligned with a vacancy in the c direction. There is more charge transfer occurring in the AA stacked region compared to the AB stacked region. The purple and yellow ball represents Mo and S atom.

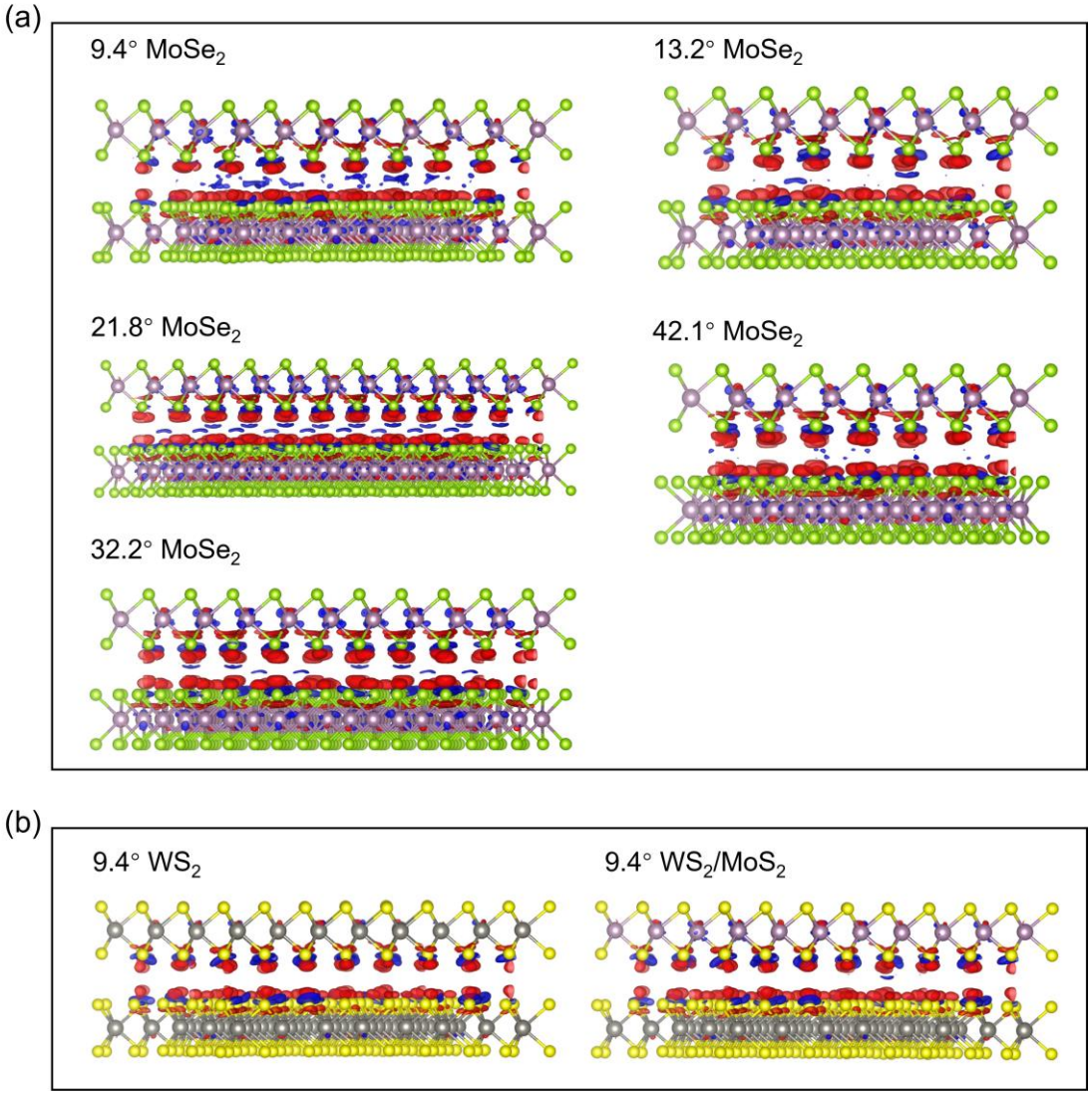

Figure S4. (a) Interlayer charge transfer of $MoSe_2$ MSLs. There are more charge accumulating in the interlayer region of 9.4° MSL compared to the MSLs with other twist-angles. (b) The interlayer charge transfer of 9.4° WS_2 and 9.4° WS_2/MoS_2. They have analogous interlayer charge density differences. The purple and gray ball represents Mo and W atom. The green and yellow ball represents Se and S atom.

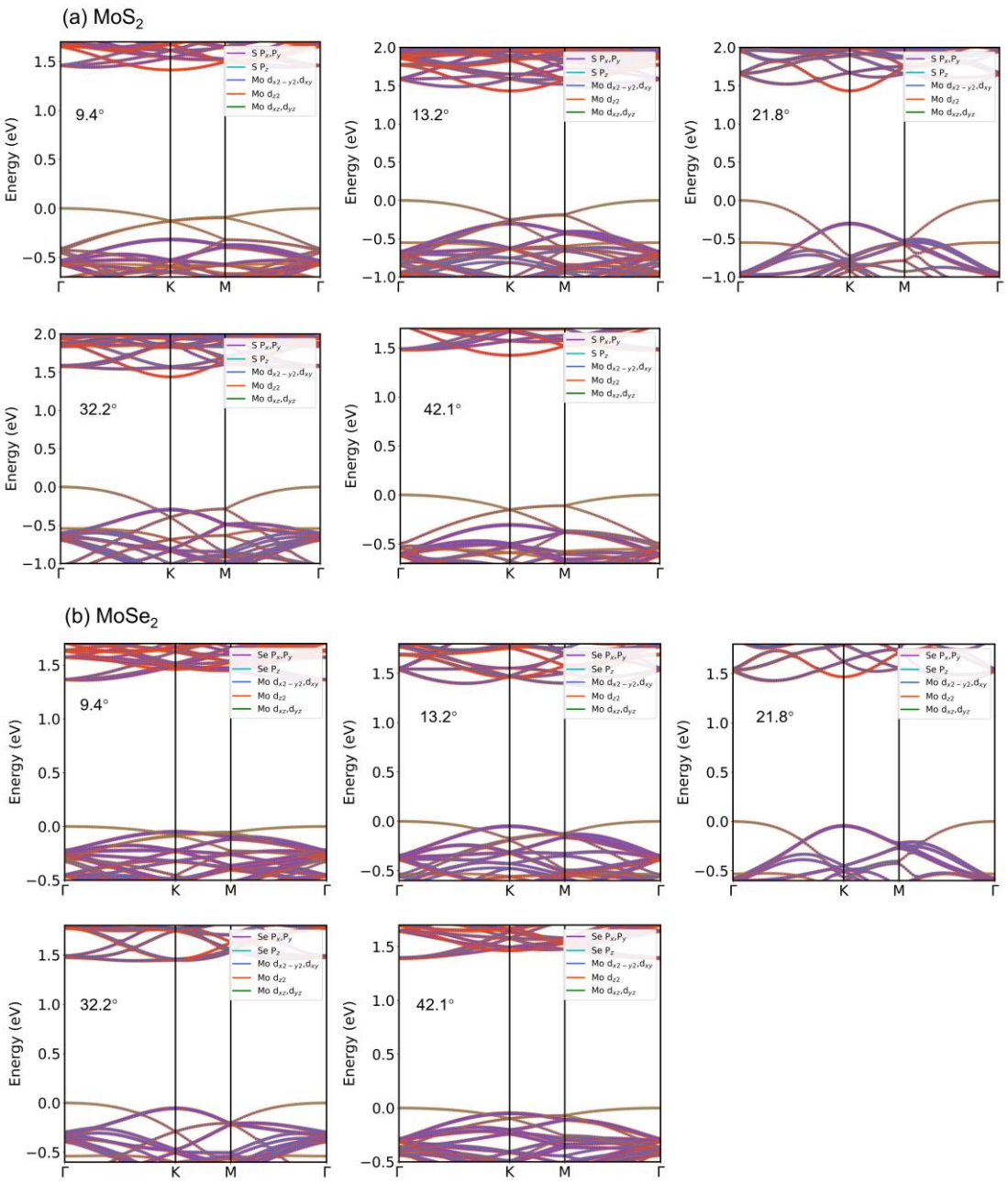
(a) MoS2
9.4°
13.2°
21.8°
32.2°
42.1°
Energy (eV)
Γ
K
M
S Px,Py
S Pz
Mo dx2 − y2,dxy
Mo dz2
Mo dxz,dyz
(b) MoSe2
Se Px,Py
Se Pz

(c) WS_2

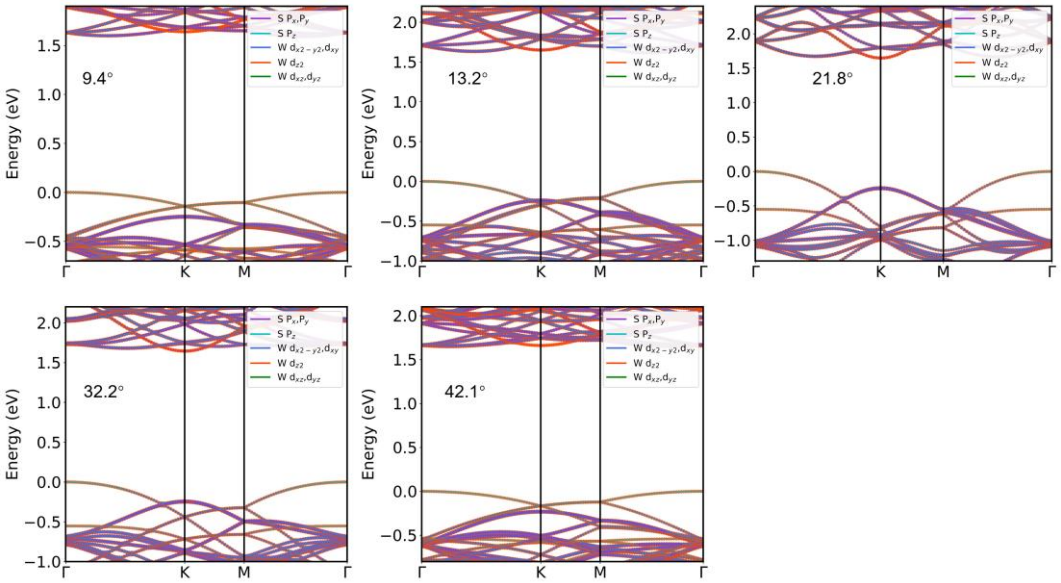

(d) $MoS_2/MoSe_2$

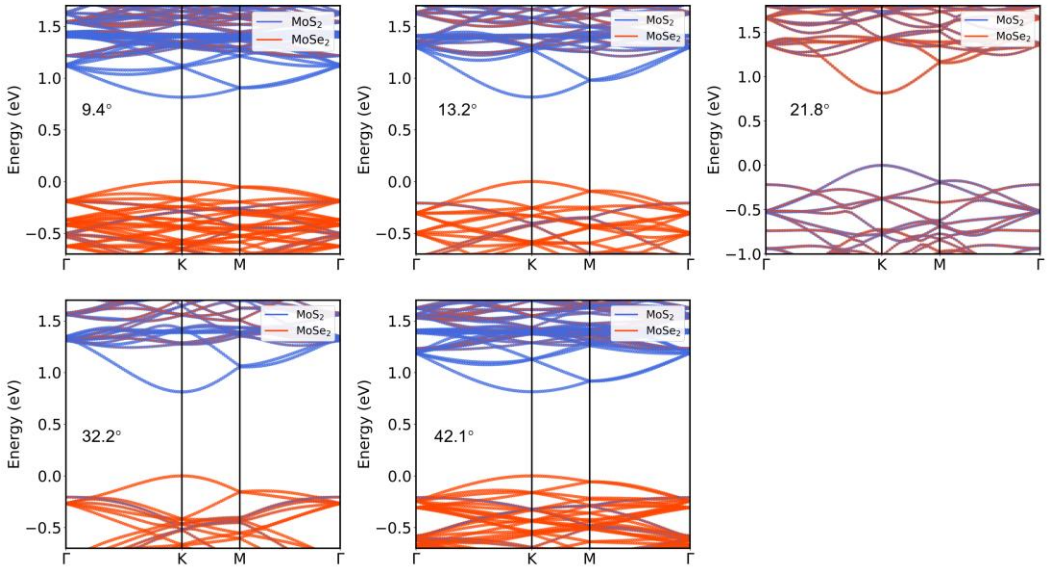

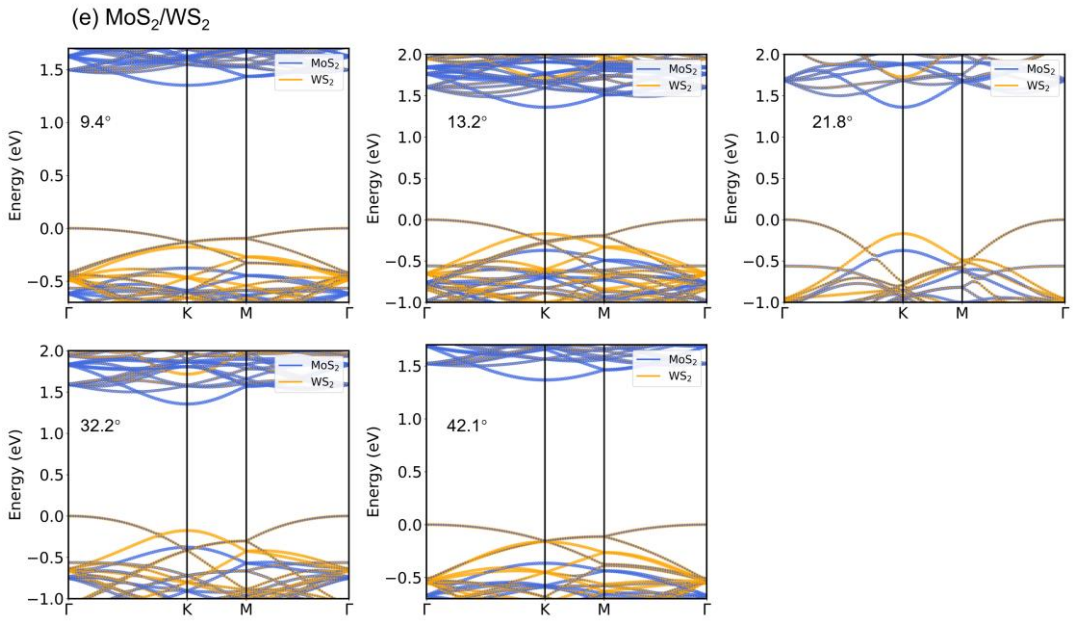

Figure S5. Projected band structure of twist-angle TMD MSLs. The contributions of atom orbital and each monolayer to the band structure of are labeled by different colors.

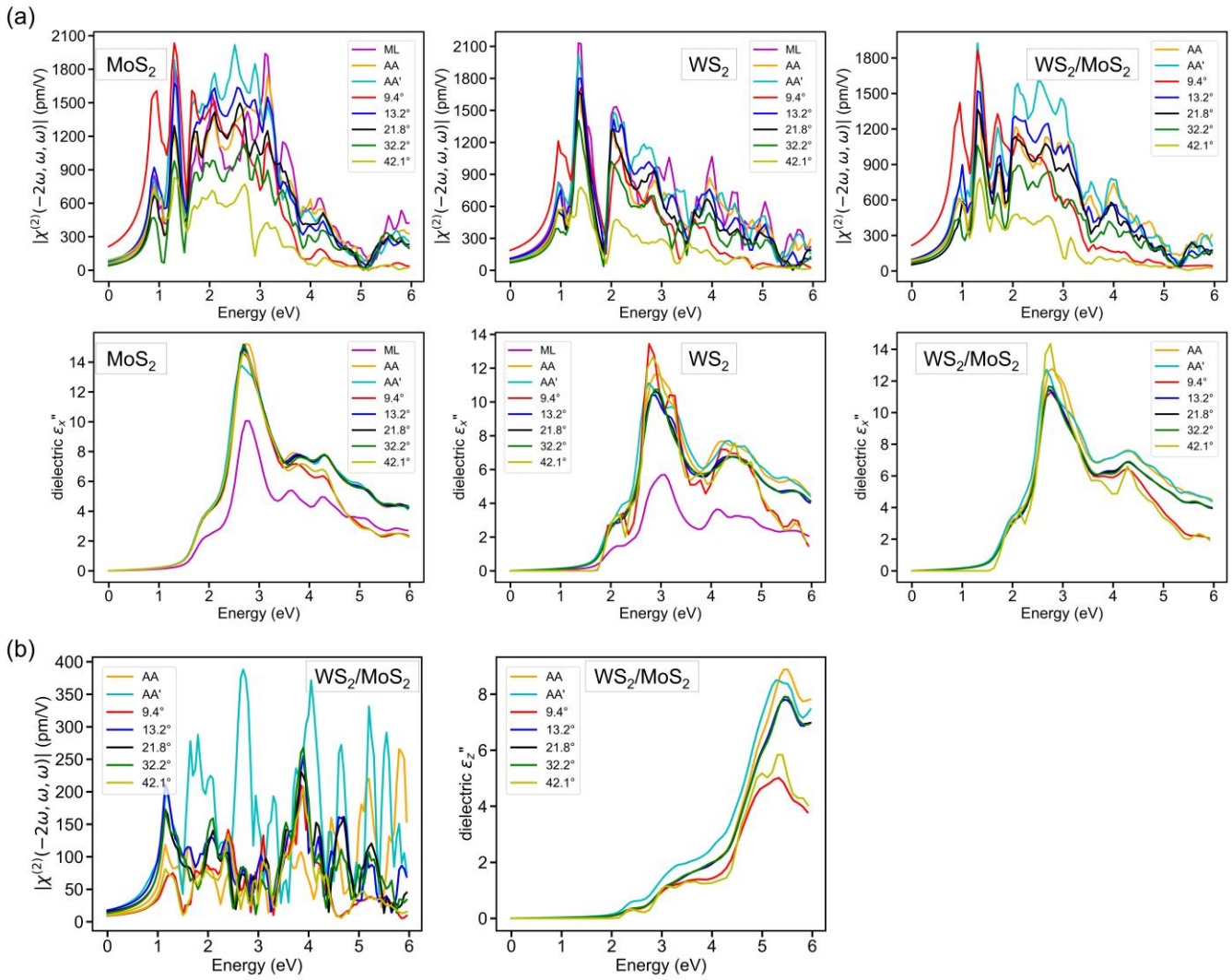

Figure S6. (a) Frequency-dependent in-plane electronic contributed SHG spectra and the imaginary part of the dielectric function along the x-direction of MoS_2, WS_2, WS_2/MoS_2 MSLs with different twist angles, and monolayer (ML), AA, AA' stacked bilayer TMDs. (b) Frequency-dependent out-of-plane electronic contributed SHG spectra and the imaginary part of the dielectric function along the z-direction of WS_2/MoS_2 MSLs with different twist angles, and AA, AA' stacked bilayer TMDs.

Table S1. Band gap values for monolayer, AA, AA' stacked TMDs and twist-angle MSLs.

Indirect band gap (eV)

	MoS_2	$MoSe_2$	$MoS_2/MoSe_2$	WS_2	WS_2/MoS_2
monolayer	1.74	1.51	\	1.89	\
AA	1.51	1.39	0.77	1.69	1.44
AA'	1.23	1.16	0.78	1.42	1.23
9.4°	1.41	1.36	0.81	1.59	1.35
13.2°	1.43	1.37	0.82	1.61	1.36
21.8°	1.43	1.42	0.81	1.65	1.36
32.2°	1.44	1.44	0.81	1.64	1.35
42.1°	1.43	1.39	0.81	1.65	1.37

Direct band gap (eV)

	MoS_2	$MoSe_2$	$MoS_2/MoSe_2$	WS_2	WS_2/MoS_2
monolayer	1.74	1.51	\	1.89	\
AA	1.72	1.48	0.77	1.87	1.53
AA'	1.66	1.45	0.78	1.81	1.60
9.4°	1.44	1.36	0.81	1.60	1.44
13.2°	1.51	1.41	0.82	1.65	1.53
21.8°	1.56	1.45	0.81	1.74	1.53
32.2°	1.57	1.47	0.81	1.73	1.53
42.1°	1.48	1.39	0.81	1.65	1.48

Table S2. Static in-plane SHG susceptibility for monolayer, AA, AA' stacked TMDs and twist-angle MSLs (pm/V).

	MoS_2	$MoSe_2$	$MoS_2/MoSe_2$	WS_2	WS_2/MoS_2
monolayer	85.7	173.3	\	125.6	\
AA	56.1	137.8	93.1	90.6	80.2
AA'	92.4	139.8	123.7	112.2	105.3
9.4°	206.0	358.5	296.6	188.2	205.7
13.2°	82.2	183.0	146.6	107.0	92.25
21.8°	40.2	104.0	89.8	80.3	64.4
32.2°	39.0	91.2	79.8	68.0	60.1
42.1°	97.9	147.2	124.2	89.6	93.73

Table S3. Static out-of-plane SHG susceptibility of $MoS_2/MoSe_2$ and MoS_2/WS_2 MSLs (pm/V).

	$MoS_2/MoSe_2$	WS_2/MoS_2
AA	53.37	11.5
AA'	95.3	17.4
9.4°	40.0	8.9
13.2°	70.9	17.6
21.8°	68.5	15.0
32.2°	70.9	13.5
42.1°	64.7	9.92

Reference

1 S. Sharma and C. Ambrosch-Draxl, *Physica Scripta*, 2004, **T109**, 128.